THERMO-CHEMICAL CONVERSION OF CIGARETTE BUTT FILTERS WASTE THROUGH PYROLYSIS PROCESS USING THERMAL ANALYSIS TECHNIQUES

Bojana BOŽILOVIĆ[a], Bojan Ž. JANKOVIĆ[b], Milena PIJOVIĆ-RADOVANOVIĆ[b], Hadi WAISI[a,c], Milena MARINOVIĆ-CINCOVIĆ[b], Sanja KRSTIĆ[b], Vladimir M. DODEVSKI[b,*]

[a]University UNION-Nikola Tesla, Faculty of Ecology and Environmental Protection, Cara Dušana 62-64, Belgrade, Serbia

[b]University of Belgrade, "Vinča" Institute of Nuclear Sciences – National Institute of the Republic of Serbia, Mike Petrovića Alasa 12-14, P.O. Box 522, 11001 Belgrade, Serbia

[c]University of Belgrade, Institute of General and Physical Chemistry, Studentski trg 12/V, P.O. Box 45, 11158 Belgrade, Serbia

[*] Corresponding author; *E-mail address*: vladimir@vinca.rs

Abstract

Thermo-chemical conversion of cigarette butt filters (CBFs) waste was investigated using various thermal analysis techniques (simultaneous TG-DTG-DTA and DSC methods) at different heating rates in an inert atmosphere. Thermo- and thermophysical properties of waste material were discussed, from the point of view of chemical structure and the influence of experimental parameters on the conversion process. It was established that acetyl groups of plasticizer (triacetin, TAC) interact with cellulose acetate (CAc) through dipolar interactions and hydrogen bonding's. Influence of these polar interactions can affect the position of glass transition temperature (T_g) of CBF. Based on estimated value of T_g from DSC analysis, it was found that CAc present in CBF has degree of substitution (DS) equals to 2.8 (DS = 2.8), where the presence of cellulose triacetate (CTA) was confirmed. It was assumed that an increase of DS leads to decline in the crystallinity. A decline of crystallinity causes the reduction of hydroxyl groups, leading to less organized chains, and whereby decreasing of inter-molecular interactions through hydrogen bonding. Based on the examination of thermophysical characteristics of the tested material, it was found that both, the heat capacity and the thermal inertia (TI) of material linearly increase with temperature, during pyrolysis progression. It was concluded that the type of bio-char produced in this process would have a large capacity to store the heat, which may depend on the formed particles size diameter and porosity. Furthermore, it was inferred that magnitude drops of thermal conductivity (κ) after T_g depends on the material fibrillation.

Key words*: industrial waste*, pyrolysis*, thermal analysis*, glass transition*, thermophysical properties*, heat-resistance*

Introduction

Large amounts of pollutants in the world threaten the humans, animals, and plants life. The World Health Organization has reported that tobacco and related products threaten many resources on the Earth. According to the World Health Organization, there are many pollutants that pose damage to the environment during the tobacco product life cycle. Although tobacco processing and production take place in particular regions of the world, its use and waste are widely dispersed around the globe. Since produced wastes can be found everywhere, their collection and disposal are considered as the complex problem. Approximately, 967 million smokers in the world used 6.25 trillion cigarettes in 2012 [1]. However, smoked cigarettes were reported to be decreased to 5.7 trillion in 2016. Considering the rapid development of this market, this rate is expected to rise up to 9 trillion by 2025 [2]. Cigarette butts (CBs) are the main residue of tobacco around the world, and they account for a large share of pollutants collected in urban clean-ups [3]. Cigarette consumption waste in the world is estimated to be 340-680 million kg. Approximately, 2 million tons of ink, paper, foil, cellophane, and glue are used for cigarettes packaging. The uncontrolled distribution of CBs is a bigger problem, because they are not biodegradable and release more than 7.000 toxic chemicals into the environment [4]. Inappropriate CBs dumping has led to a number of domestic and wildland fires, with disastrous consequences. Many countries ratify some rules against using tobacco and advocate the policies on raising the price of the tobacco-based product [5]. Considering the inefficiency of conventional disposal techniques, such as landfilling and incineration, which are not feasible for CBs, an effective solution for management and disposal of this waste seems to be essential. An efficient disposal method for this waste could reduce the release of toxic chemicals into the environment and lead to some benefits, such as energy supply from the huge volume of waste material. There are several methods for recycling and reusing the CBs to ensure a hazardless procedure for their life cycle. CBs are mainly made up of *cellulose acetate* (CAc), which has attracted the attention of many researchers. A single cigarette filter contains about 12.000 fibers of CAc [6]. These fibers consist titanium dioxide (TiO_2) and they are connected together by a *triacetin* (TAC) (glycerol triacetate) surfactant (*plasticizer*) [7]. The molecular formula of CAc is $C_{76}H_{114}O_{49}$ with average molecular weight of 1.811,7 $g \cdot mol^{-1}$ [8]. The high amounts of carbon (C) atoms in the CAc structure makes it a good candidate to be used as the raw material for producing the porous carbon derivatives. The primary element of CBs, the CAc, is a desirable organic carbon source for its conversion into useful liquid finished goods using thermal cracking techniques [9]. The pyrolysis approach has been successfully used for decomposition of cellulose to furan [10], carboxylic acid and aldehydes [11], and hydrocarbons/aromatics [12]. The main target of these conversions is to achieve sustainable energy from waste. The liquid fuel produced by pyrolysis can be used as a fuel oil in static heating and applied for electricity generation. Interestingly, pyrolysis can directly produce a liquid fuel, which is a good option, when the resources are far from the energy-required place. Pyrolysis process has received much attention due to its ability to produce high amount of liquid oil (~ 80 wt.%) at moderate temperature of about 500 °C. Moreover, it is very flexible as its parameters can be manipulated to optimize the product yield, based on preferences. The oil produced by the biomass pyrolysis is considered as a highly environmentally friendly fuel, because it contributes to the reduction of CO_2 in an atmosphere [13]. Many studies have focused on the risk of CBs being released into the environment, but a much smaller number of studies have been done on the converting of CBs into valuable products, *via* the pyrolysis process. In order to be as familiar as possible with the described conversion process of this type of waste, we need to know more about the structure of CBs.

CB is a cigarette filter which has some tobacco with some chemical compounds and contaminants. The key material used in CBs is *cellulose acetate* (CAc), which is resistant to biodegradation compounds, and remains un-degraded in the environment for 18 months in the usual conditions [14]. To create a cigarette cartridge, TiO_2 is exposed to the cellulose acetate fibers with a thickness of about 20 mm and 15.000 of them are densely packed along with TAC as a binder [15]. In addition, metal ions are among the most significant pollutants discovered in CBs and they can cause pollution in the aquatic species, if discharged into the marine ecosystems [16]. The value of heavy metal ions, such as arsenic, nickel, cadmium, lead, zinc and copper, in CBs is known to be from some $\mu g \cdot g^{-1}$ to many hundred $g \cdot g^{-1}$ [17]. Also, the CBs have a capability to release polycyclic aromatic hydrocarbons (PAHs), which can cause cancer in the living organisms in the ecosystem. CBs also include polycyclic aromatic compounds (PACs) such as nicotine, which have an adverse effect on humans [18].

Researchers efforts to recycle CBs were influenced by the physical structure and chemical properties of CBs. CB recycling processes are examined in brick manufacturing, the cement production, mosquito handling, porous carbon and absorbent production, voice insulating materials, paper performance, and biofilm drivers in wastewater treatment. CB refining is not requiring in some fields such as bricks or asphalt manufacturing, and cigarette could be used in the original form. The CB, however, needs to be processed by extraction procedure, pyrolysis, and filter rod extraction for the other purposes. Reuse of CBs in various mechanisms can contribute to the production of functional items. It was proved that CBs contain a number of recyclable materials owing to

their *physicochemical properties*. Since CAc is the key constituent of CBs, it was applied to manufacture nano-crystalline cellulose [19] and the cellulose-based membranes [20]. CBs treatments included several effective opportunities to recover them. Nevertheless, the CBs have always been a solid waste despite being utilized as *absorbent* products. Moreover, these recycled products need to be further destroyed to prevent the production of solid contaminants in an area. The CAc is a highly efficient natural carbon source and could be processed into highly valued liquid fuels, using the efficient thermochemical processing, such as *pyrolysis*. The pyrolysis process has been widely used for the conversion of cellulose to hydrocarbons/aromatics, furan substances, and other organic materials such as aldehydes, carboxylic acids and similar compounds [11]. Pyrolysis is a thermal disintegration of compounds, where there is no oxygen or slightly less oxygen full combustion. A precise description of pyrolysis is difficult, particularly when it is applied to biomass. Earlier studies typically correlate pyrolysis with the carbonization process, of which a solid char is a primary ingredient. The term pyrolysis defines processes, where the oils are favored products. The pyrolysis method may be divided into various types according to the configurations of the process. The "*fast pyrolysis*" refers to heating carbon-based materials at a heating rate of 100-1300 °C·s^{-1} for 1 s to 10 s. This process is typically applied for producing bio-oil, because pyrolysis process oil content is significantly higher than the char and gas output. Consequently, 60-75% liquid bio-oil, 10-20% volatile gas compounds, and 15-20% bio-chars are common commodity yields in rapid pyrolysis [21]. The primary target of the rapid pyrolysis procedure is to heat carbon-based feedstock to reach the thermal decomposition, thus shortening the release time and facilitating the char forming. The standard form of pyrolysis is the slow pyrolysis, which usually requires low levels of heating and high periods of residency. The slow pyrolysis cycle favors carbonaceous char output but liquid, while the gas fuel compounds are often generated, in comparatively limited amounts [22].

This study is focused on the slow pyrolysis of cigarette butt filters (CBFs) using thermal analysis techniques (thermogravimetry – TG, derivative thermogravimetry – DTG, differential thermal analysis – DTA, and differential scanning calorimetry - DSC) aiming to develops the valuable items, such as releasing performance of volatiles (the devolatilization index, D_i), then the heat-resistance index (HRI) (the value used to evaluate the thermal resistance of the polymer material), the temperature transition properties (the evaluation of glass transition temperature T_g, by the DSC, in order to determine the thermal behavior of the complex blend), the temperature dependence of the specific heat capacity, c_p, of the investigated waste material (neglecting its crystalline melting), as well as its thermal inertia (TI) (quantity closely related to thermal conductivity, density and the heat capacity of tested material). All mentioned quantities were determined and discussed in order to gain a deeper understanding of the thermal stability of this type of waste, for its recycling into valuable by-products, during a thermally induced processes under the inert conditions.

Materials and methods

Sample preparation

Collected cigarette butts (CBs) from the same manufacturer (the same cigarette brand from USA Company) were used as raw material. CBs were cleaned on the cardboard from the ash obtained by burning of tobacco and from unburnt tobacco which was remained. Subsequently, the cigarette filters (CFs) (which are previously unwrapped from the paper) which are primarily cellulose acetate (CAc) fibers are mechanically separated from the rest of CBs (*note*: separation of filters from the ash, the remaining tobacco and the paper was performed by the hand) (all CFs produced in USA are made up of cellulose acetate (CAc) which is a *plastic product*; each filter consists of around 12.000 CAc fibers and these fibers contain delustrant, titanium dioxide (TiO$_2$), as well as triacetin (TAC) (glycerol triacetate) which is added to the fiber as the fiber binder (*plasticizer*)). Therefore, without any pretreatment, coated papers of butts are carefully removed to isolate the filters themselves. Thereafter, fibrils were chopped with scissors into smaller pieces and then put in a mill, where they were further grounded.

TG-DTG-DTA and DSC measurements

Slow pyrolysis was performed by the simultaneous non-isothermal thermogravimetry (TG) – derivative thermogravimetry (DTG) and differential thermal analysis (DTA) using a SETARAM SETSYS Evolution 1750 instrument (7 Rue de l'Oratoire, 69300 Caluire-et-Cuire, France). High purity argon (Ar) gas (99.999 %; SETARAM SETSYS) was used as protective atmosphere. The samples with mass of approximately ~ 6 mg were heated at three different heating rates, β = 10 K/min, 20 K/min and 30 K/min, in an argon (Ar) atmosphere (with gas flowing rate of φ = 20 mL min^{-1}), in a temperature range from 30 °C up to 700 °C. To minimize air contact of the sample during its inserting, the oven environment of thermogravimetric analyzer and the oven interior were permanently flushed with Ar (~ 80 mL min^{-1}). The duplicate non-isothermal runs were performed under similar conditions and data were found to overlap with each other (including control measurement for each heating rate used, with approximately the same sample mass), indicating satisfactory reproducibility. Each

run was carried out in duplicate, in order to minimize an experimental error. Experimental TG-DTA tests were performed according to comprehensive calibration and measurement procedure that precedes the sample measurement, and it is defined by an equipment manufacturer in order to handle the reproducibility and re-productivity of output results. The calibration procedure was performed according to the manufacturer's instructions and measurements with empty corundum crucibles, in order to correct the measured signals, and handle the mass balance deviations. Those are common procedures for this type of the experimental setup, which guarantee the accuracy of measurements, declared by the equipment manufacturer - SETARAM. In addition to thermal characterization of a given material, TA Q1000 DSC Tzero™ (Thermal Analysis Instruments - TA Instruments LTD, 159 Lukens Drive, New Castle, DE 19720, USA) equipment (which operates in the temperature range of $\Delta T = -180$ °C – +725 °C with sensitivity of 0.2 µW, where calibration is carried out *via* the instrument control software) was used, for determination of glass transition temperature (T_g). The DSC test was performed with a mass of the sample of ∼ 3.30 mg at the heating rate of $\beta = 10$ K/min, and under an argon gas (Ar) atmosphere (the purge and the protective gas were $\varphi = 20$ mL min^{-1}) to avoid any oxidation reactions. DSC measurement was conducted through a double scan mode from +21 °C to +377 °C, where T_g point is estimated using mid-point curve approach, within an detected sensitive DSC-signal changes. This procedure is important, considering that usefulness of CAc can be strongly influenced by its decomposition process and stabilization properties.

Thermal stability indexes

For describing the release of volatiles quantitatively, the devolatilization index (D_i) was calculated in accordance with equation (1) [23]:

$$D_i = \frac{R_{max}}{(T_{in}T_{max}\Delta T_{1/2})},$$ (1)

where R_{max} is the maximum decomposition rate (in %/min), while T_{in} and T_{max} are the initial devolatilization temperature and the maximum mass loss temperature, respectively; $\Delta T_{1/2}$ represents the temperature interval when the value of R/R_{max} was ½ (i.e., when the instantaneous mass loss rate equals to the half of R_{max}). Devolatilization index (D_i) is determined by highest mass loss rate where the decomposition is the largest, regarded as a measure to evaluate the pyrolyzability of samples under investigation. The higher D_i value generally indicates easier devolatilization process and better pyrolyzibility performances. The second quantitative index related to evaluation of considered process, represents an heat-resistance index (HRI) [24]. The heat-resistance index was the value used to evaluate the thermal resistance of polymer based sample. The HRI index can be calculated by the following formula:

$$T_{HRI} = 0.49 \times [T_5 + 0.6 \times (T_{30} - T_5)],$$ (2)

where T_5 and T_{30} are defined as temperatures at 5% and 30% of mass losses, respectively, and these temperatures can be extracted from TG experimental data. If T_{HRI} value rises as the heating rate (β) increases, this is indication that the thermal resistance increases with an heating rate.

Thermal properties of the sample in dry state

Given the potential instability of investigated material, however, it is imperative to understand the aging mechanisms and deterioration pathways of cellulose ester plastics (*apropos* the cellulose acetate (CAc) in cigarette filters) to mitigate decomposition and formulate guidelines for CFs exhibition and recycling. One important aspect of this process is the ability to fully thermally investigates this *micro-plastic*, because variations in composition affect its aging properties and the ultimate stability.

The free molecular motion of the main chain of cellulose is restricted due to inter-molecular hydrogen bonding. Cellulose is insoluble in water, however, it sorbs a characteristic amount of water. Since the hydroxyl groups form hydrogen bonding with water molecules, it is difficult to obtain completely dry testing samples. The thermal peak related to vaporization, depends on the amount of water. Not only for cellulose, but also natural polysaccharides show no first order phase transition, if they are in the dry state. However, the rate at which heat is transported and stored in polymers in a flame or fire is of the fundamental importance, because these processes determine the time to ignition and burning rate. These processes are very important when evaluating the duration of material decomposition, during its thermo-chemical conversion into other, an value-added materials.

There are no good theories to predict the thermal conductivity κ (W·m^{-1}·K^{-1}), the specific heat capacity c_p (kJ·kg^{-1}·K^{-1}), or density ρ (kg·m^{-3}) of condensed phases (e.g., the solid or molten polymers), but empirical structure-property correlations have been developed that allow the estimation of thermal properties from

additive atomic, or chemical group contributions, if the chemical structure of the plastic is known. The rough approximation of temperature dependence of the thermal conductivity relative to its value at the glass transition temperature (T_g), $\kappa(T_g)$, can be expressed as [25,26]:

$$\kappa \approx \kappa(T_g)\left(\frac{T}{T_g}\right)^{0.22} for\ T < T_g \tag{3}$$

$$\kappa \approx \kappa(T_g)\left[1.2 - 0.2\left(\frac{T}{T_g}\right)\right] for\ T > T_g. \tag{4}$$

The relationship between density and temperature can be expressed (neglecting the abrupt change on melting of semi-crystalline polymers) to the first approximation [25,26]:

$$\frac{1}{\rho} = \frac{1}{\rho_o} + B(T - T_o), \tag{5}$$

where $\rho = \rho(T)$ is the density at temperature T, ρ_o is the density at temperature of $T_o = 298$ K and $B = 5 \pm 2 \times 10^{-7}$ $m^3 \cdot kg^{-1} \cdot K^{-1}$ is the volume thermal expansivity. Neglecting crystalline melting, the temperature dependence of the heat capacity can be approximated as [25,26]:

$$c_p = (c_o + \Delta c_p) \cdot (0.64 + 1.2 \times 10^{-3}T) \approx 0.75 c_o(1 + 1.6 \times 10^{-3}T) \tag{6}$$

where $c_p = c_p(T)$ in units of $kJ \cdot kg^{-1} \cdot K^{-1}$ is the heat capacity at temperature T, c_o is the heat capacity at standard temperature, $T_o = 298$ K, and Δc_p is is the change in heat capacity at the glass transition temperature. Additionally, the product $\kappa \cdot \rho \cdot c_p$ is the quantity called the *thermal inertia* (TI), which emerges from the transient heat transfer analysis of the ignition time. The individual temperature dependence of κ, ρ, and c_p revealed by equations (3) – (4) through equation (6) and the experimental data for about a dozen plastics [25,26], suggest that the product of these terms (i.e., the thermal inertia, TI) should have the approximate temperature dependence, such as:

$$\kappa \cdot \rho \cdot c_p(T) \approx \kappa_o \cdot \rho_o \cdot c_{p(o)}\frac{T}{T_o} = (\kappa \cdot \rho \cdot c_p)_o \frac{T}{T_o}, \tag{7}$$

where κ_o, ρ_o and $c_{p(o)}$ are the room temperature (RT) (T_o) values listed in Table 1 for cellulose acetate matrix polymer in CFs.

Table 1. Thermal properties of cellulose acetate (CAc (CA)) at $T_o = 298$ K

Polymer	κ [W·m^{-1}·K^{-1}]	ρ [kg·m^{-3}]	c_p [kJ·kg^{-1}·K^{-1}]
CAc	0.25	1250	1.67

Glass transition of cellulose acetates with various degrees of substitution (DS) and the molecular mass

Cellulose acetate (CAc or CA) is ordinarily prepared from wood pulp by acetylation in acetic acid and sulfuric acid. Chemical structure of CAc (or CA) is shown in fig. 1.

Cellulose Acetate (CA)
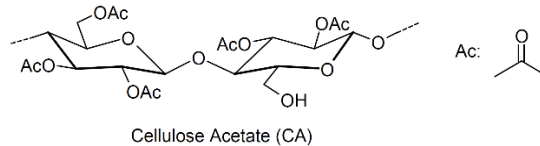
**Figure 1. Cellulose acetate (CA) chemical structure (Ac: acetate group)**

Degree of substitution (DS) is defined as the number of the acetyl groups substituted from the hydroxyl group. As an industrial index, CA samples with DS ranged from 2.40 to 2.56 are designated as cellulose

5

diacetate (CDA) and those from 2.80 to 2.92 as cellulose triacetate (CTA). The C_6 position is preferentially substituted, and the substitution of C_2 and C_3 occurs statistically. In addition, when the molecular mass of CA increases, the thermal decomposition starts immediately after completion of melting or the glass transition [27]. The T_g increases with an increasing of the molecular weight. When the DS decreases, T_g maintains a constant value, regardless of the molecular weight of the polymer [28]. Therefore, when DS decreases, T_g maintains the constant value regardless of molecular weight, and *only depends on degree of substitution - DS*. With increasing DS, T_g decreases due to the expansion of inter-molecular distance.

Results and discussion

Thermal analysis profiles of pyrolysis process regarding the micro-scale experiments

Simultaneous TG-DTG curves for devolatilization process of cigarette butt filters (CBFs) at 10 K/min in an argon (Ar) atmosphere are plotted in fig. 2 A.

A

C

B

D
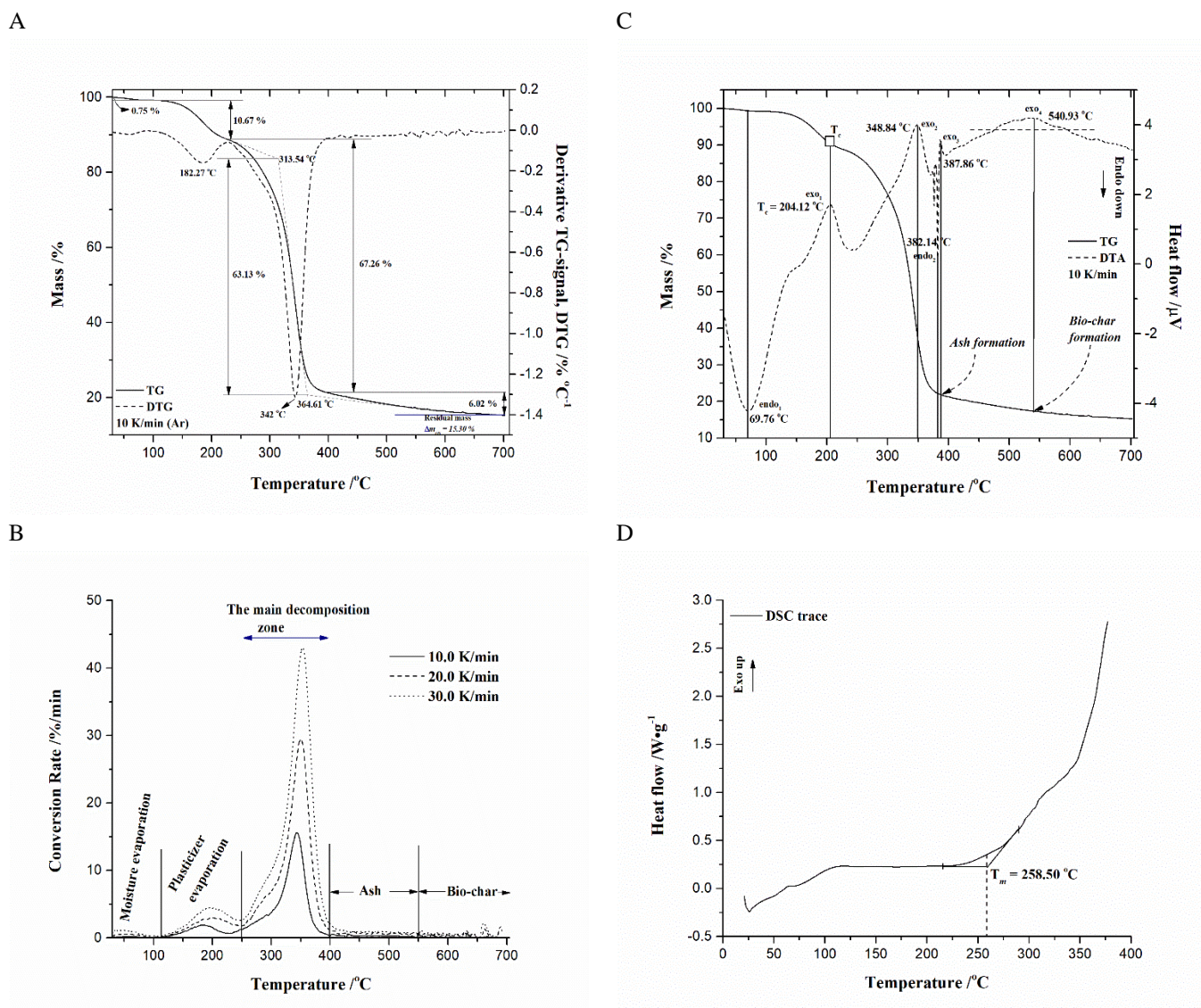
Figure 2. A. Simultaneous TG-DTG curves at 10 K/min, with marked characteristic temperatures and sample mass losses at given process stages (the residual mass was also designated). B. Conversion (absolute) rate curves (%/min) at various heating rates (β = 10, 20 and 30 K/min) with marked reaction phases during thermo-chemical conversion. C. Simultaneous TG-DTA curves at 10 K/min, with marked thermal effects during thermo-chemical conversion process (the reaction point-check temperatures were designated). D. DSC curve of CBF sample at the heating rate of β = 10 K/min, measured in the temperature range of ΔT = +21 °C - +377 °C. The position of the melting temperature (T_m) is indicated (T_m = 258.50 °C)

It can be seen from fig. 2 A, that there is a small sample mass loss of approx. ~ 0.75 % with a slight inclination on the DTG curve below 100 ^{o}C, which can be attributed to moisture evaporation (desorption), accumulated on the surface of the sample. After that, there is a significant mass loss (~ 10.67 ^{o}C) manifesting as a DTG peak at 182.27 ^{o}C (fig. 2 A), and this reaction stage is attributed to the thermal decomposition of plasticizer, which is present in the filter production [29]. In the third reaction stage, there is the largest mass loss of the sample of ~ 63.13 %, and represents the main decomposition stage. This stage is characterized by a DTG peak located at temperature of 342 ^{o}C, which is attributed to the thermal decomposition (pyrolysis) of cellulose acetate (CAc) [30]. Namely, it can be assumed that initial decomposition temperature of CAc is 313.54 ^{o}C and maximum mass loss rate temperature is 364.61 ^{o}C, where the mass loss between them amounts ~ 67.26 % (fig. 2 A). In the fourth reaction stage, the sample mass loss is ~ 6.02 %, with residual mass of ~ 15.30 % at 700 ^{o}C (fig. 2 A). The actual stage is characterized by processes of ash formation and formation of the carbon residue (bio-char). All thermo-chemical conversion stages of investigated material are clearly marked on corresponding conversion rate (*absolute*) curves, as a function of process temperature at various heating rates (fig. 2 B). Based on the position of peaks appeared on the conversion rate curves, it seems that pyrolysis step related to plasticizer decomposition shows a certain dependence on the heating rate. On the other hand, conversion peaks located inside the main decomposition zone show moderately dependence on the heating rate. The maximum temperature peak shifts are in properly order with an increasing of heating rate (where the reaction rate also increases) in the *T*-range between 300 ^{o}C and 400 ^{o}C, where deacetylation reaction occurs [31]. The charring process takes place at higher temperatures above approx. ~ 550 ^{o}C, highly dependent on CAc degradation reactions. Further, by increasing the temperature above 600 ^{o}C until the very end of the process, the carbon yield amounts ~ 15 %, when actual material is subjected to the pyrolysis process [32]. According to Koochaki et al. [33], the mass loss observed up to 250 ^{o}C can be related to evaporations of free water (connecting to the surface of the raw material) and added plasticizer (fig. 2 B). After that there is a mass loss which includes *T*-range between 250 ^{o}C and 400 ^{o}C, related to the decomposition of hemi-cellular components of raw material. Finally, there is a slow mass loss by increasing the temperature up to 700 ^{o}C (figs. 2 A and B), which belongs to cracking reaction of C–C bonds (the slower step). Comparative analysis of physicochemical phenomena derived from TG and DTA recording closely related to thermal decomposition, can give more detailed information about thermal effects that then occur. This is important, considering thermal properties of both, plasticizer and CAc present in the CBFs. The appropriate simultaneous TG-DTA curves for pyrolysis (devolatilization) process at β = 10 K/min are shown in fig. 2 C. From presented DTA scan, there are both exothermic and endothermic effects during decomposition process. Namely, broader endothermic peak (endo$_1$) located at 69.76 ^{o}C is attributed to water (H_2O) desorption from polysaccharide structure. With an increase in the temperature, at a position of T ~ 204.12 ^{o}C, the exothermic event (exo$_1$) appears (fig. 2 C), and this can be attributed to CAc crystallization (marked as T_c) [34,35]. This event suggests that the part of the material can be crystallized under appropriate conditions, and it is clear indication for the change in degree of substitution (DS) [35]. Namely, DS of the polymer represents the (*average*) number of substituent groups attached *per* base unit (in the case of condensation polymers) or *per* the monomeric unit (in the case of addition polymers). This term is usually used in cellulose chemistry, where each anhydroglucose (β-glucopyranose) unit has three reactive (hydroxyl) groups. The DS can therefore range from zero (cellulose itself) to three (fully substituted cellulose). In the case of CAc, the DS is the average number of acetyl groups attached *per* anhydroglucose unit. In total perspective, the eight possible anhydroglucose units (AGU) of CAc may occurs. So, for our investigated filter, we are dealing with a typical cellulose derivative, where there is substitution of hydroxyl groups of cellulose by other functional groups (by acetate). Accurate determination of DS for our sample, will be presented in next lines, related to estimation of the glass transition temperature (T_g). It should be pointed out, that observed exothermic event take place in the temperature range, where the plasticizer evaporation occurs. Namely, the plasticizer is incorporated into the amorphous parts of polymers, while the structure and size of any crystalline part remains unaffected. From plasticizer is expected to lower the T_g, to reduce the modulus, tensile strength, hardness, density, etc. It is a low molecular weight (low-MW) chemical compound, which specifically interacts with polymers, and spread them apart in order to increase a free volume in one system. Added plasticizer reduces polymer-polymer bonding and can provides more molecular mobility for macromolecules. By further increasing the temperature, it is observed the second, broad exothermic event (exo$_2$), placed at the temperature point of ~ 348.84 ^{o}C (fig. 2 C), which can be an indication of secondary crystallization arrangement, and also on the recombination of hydrogen bonding [35]. The shape of this exothermic peak is dependent on the extent of the modification of the CAc structure. In any case, it must be pointed out that acetyl groups of TAC are supposed to interact with CAc

via dipolar interactions and hydrogen bonding's. The influence of these polar interactions could affect the T_g value.

At the temperature of 382.14 ^{o}C, a sharp and narrow DTA peak appears, indicating on the endothermic event marked as endo$_2$. This transformation indicates on the melting of the acetylated sample. At this point, we come to an important crossroads, where it is obvious that the material melting overlaps with its decomposition process. Reactions that indicate these phenomena take place in a narrower temperature range, but it is largely depends on DS which real exists. According to these results, the realization of competitive fusion phenomenon of crystallized material and decomposition of cellulose derivative may occur. At the temperature position of ~ 387.86 ^{o}C, immediately after previously discussed transformation, it appears an exothermic event (exo$_3$), which can be attributed to the ash formation (fig. 2 C). Within a framework of this reaction phase, an appropriate amount of metals and inorganic fractions remaining in CBFs accumulates in the form of ash, and can be called as the metal "*contaminants*". There is accumulation of alkali and alkaline earth metals in the form of carbonates and chlorides [36], as well as an existence of thermally stable TiO$_2$. The last phase was characterized by broader exothermic effect, located at ~ 540.93 ^{o}C (as exo$_4$, fig. 2 C), where bio-char is formed. The presence of metals and especially TiO$_2$ being, can have a catalytic effect on the fabrication of final solid product, acting on the morphology and surface properties of obtained carbon through the pyrolysis process of CBFs.

Determination of the glass transition temperature (T_g) by DSC testing

The DSC test of CBF sample was used in order to determine the glass transition temperature (T_g) through the mid-point curve method, within a detected sensitive DSC-signal changes described previously (the section "*Materials and methods*"). Fig. 2 D shows the DSC trace at the heating rate of β = 10 K/min, measured in the temperature range of ΔT = +21 ^{o}C – +377 ^{o}C. From recorded DSC curve, the melting temperature (T_m) was determined through the cross-section tangents approach. For the investigated sample, the T_m value of 258.50 ^{o}C was obtained. The estimated T_m value lies a little outside of the melting temperature range for commercial CAc (CA) with an acetylation content of approximately 40 %, and plasticized with glycerol triacetate (~ 230 ^{o}C – 250 ^{o}C) [37]. A more reliable retrieval of T_m value from DTA measurements is difficult to determine, bearing in mind the above-presented discussion, while T_m and T_g values are most often determined by DSC technique, but this technique is not so precise in comparison with, for example, DMA (Dynamic Mechanical Analysis) technique. However, from presented DSC experimental testing, the visible T_g point cannot be detected (fig. 2 D). As a consequence of this fact, CAc has the narrow temperature window between its T_g value, and its decomposition temperature value. The temperature position where T_g will appears depends on the type and concentration of plasticizer. Applying the procedure described in "*Materials and methods*" section, the enlarged portion of DSC trace, where sustained sensitive DSC-signal changes are detected, is shown in fig. 3.
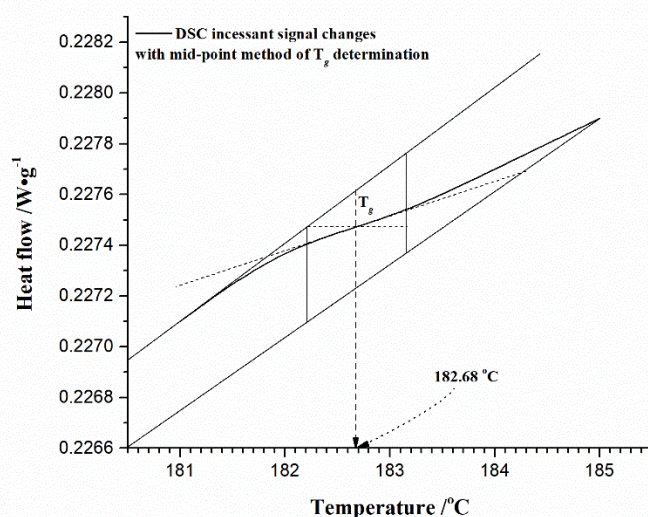
Figure 3. Procedure of the glass transition temperature (T_g) determination, for the CBF sample

8

The procedure for determining T_g, according to the described method, is shown schematically in the same figure. Based on the current investigation, the T_g is determined and amounts T_g = 182.68 °C (fig. 3). The estimated value of T_g corresponds to CAc with degree of substitution (DS) equal to 2.8 (DS = 2.8), so, it can be supposed that we have an cellulose triacetate (CTA). T_g is an important, considering interpretation of the term miscibility, between the components (CTA and TAC). The sharp T_g transition in the single-point was not observed in our case, which is characteristic for miscible blend, but related for T_g's of both components. In actual case, there is a broadening of T_g transition, which is characteristic for heterogeneous dispersion of components in the blend. It should be mentioned that T_g of DS = 2.5 exhibits value of 190 °C [29], while in our considered case, T_g value amounts 182.68 °C, so, it is lowered for 7.32 °C, increasing the degree of substitution up to 2.8. In addition, the reduction in T_g value has a need for larger amount of plasticizer (~ 30 – 40 wt.%), which would be incorporated into CAc formulation [29].

Thermal stability and devolatilization indexes of CBFs in the course of pyrolysis process

Table 2 lists the values of D_i index and the heat-resistance index (HRI) at different heating rates (β = 10, 20 and 30 K/min) considering CBF pyrolysis process. The appropriate quantities attached to D_i refer to the main decomposition zone designated on the absolute conversion rate curves (fig. 2 B). On the other hand, the appropriate quantities attached to T_{HRI}, are derived from the experimental TG curves.

Table 2. Devolatilization indexes (D_i) and heat-resistance indexes (T_{HRI}) at various heating rates related to the main thermal decomposition zone; Values of R_{max}, T_{in}, $\Delta T_{1/2}$, T_5 and T_{30} were also included

| β (K/min) [*]	R_{max} (%/min) [a]	T_{in} (°C) [a]	$\Delta T_{1/2}$ (°C) [a]	D_i (%·min⁻¹·C⁰⁻³)	T_5 (°C)	T_{30} (°C)	T_{HRI} (°C)
10	15.5	226.52	37.58	5.324×10^{-6}	172.62	315.77	126.67
20	29.6	245.62	39.70	8.673×10^{-6}	179.99	322.17	130.00
30	43.0	249.46	43.00	1.136×10^{-5}	181.94	325.14	131.25

[a] Determined from the absolute conversion rate curves (Figure 2 B). [*] The following values of T_{max} were obtained: $T_{max(1)}$ = 342 °C, $T_{max(2)}$ = 350 °C and $T_{max(3)}$ = 353 °C, for β = 10 K/min, β = 20 K/min and β = 30 K/min, respectively.

From the results presented in Table 2, it can be observed that with an increasing of heating rate, both T_{in} and $\Delta T_{1/2}$ moves to higher values, so that, elevating them to higher temperature region. With increasing of heating rate, the D_i value becomes higher and thus, the volatile release is much easier. Therefore, D_i increases with an increase in the heating rate, indicating that the higher heating rate promotes release of volatiles. This should be expected in the temperature range, where the endothermic peak endo$_2$ occurs (fig. 2 C), since that devolatilization reaction is an endothermic process, while the formation of bio-char is an exothermic process. Namely, the higher heating rate decreases residence time of the sample at lower temperature, and increases residence time at higher temperature, correspondingly. Therefore, from the perspective of reaction equilibrium, an increase of the heating rate, is conducive to inhibiting condensation reaction and promoting the devolatilization reaction (also, with an increasing of the heating rate, the maximum decomposition rate, R_{max}, is accelerated, and shifts to higher temperatures (Table 2), mainly caused by thermal hysteresis effect; the system is easier decomposed at higher temperatures, so the values of R_{max} and D_i increase. Additionally, the thermal stability of the sample was determined by TG, through the determination of T_5, T_{30} as well T_{HRI} quantities, respectively. Both values, T_5 and T_{30}, raises with heating rate elevating, but these values strongly depends on DS. Namely, decomposition temperatures, T_5 (Table 2), are smaller than those associated with precursor sample with a lower DS values [38]. Namely, it was found that the onset decomposition temperature for the cellulose triacetate (CTA) sample with DS = 2.92 amounts 252 °C [27], so, we can see that T_{in} values (Table 2) are very close to indicated one, and consequenty these values are highly appreciated for our investigated sample, with DS ~ 2.8. This is closely related with crystallinity index of the sample. Hence, with an increase of DS, the crystallinity decreases. In that sense, the decrease of crystallinity for our sample (i.e., semi-crystallinity behaviour) indicates on the reduction of hydroxyl groups, leading to less organization of the chains, decreasing an inter-molecular interactions through hydrogen bonding, and thus decreasing the crystallinity. Mentioned facts are also reflected in the values of heat-resistance index (T_{HRI}) (Table 2). Based on this discussion, acetyl groups

decrease the intensity of the formation of hydrogen bonds and lower temperatures (Table 2) are therefore needed for the beginning of the event of glass transition temperature – T_g (see previous sub-section).

Thermophysical properties of CBFs during pyrolysis

Figs. 4 A and B show the temperature dependence of c_p and TI (the thermal inertia) of the CBF sample, during thermo-chemical conversion, within the observed experimental temperature range.

A   B
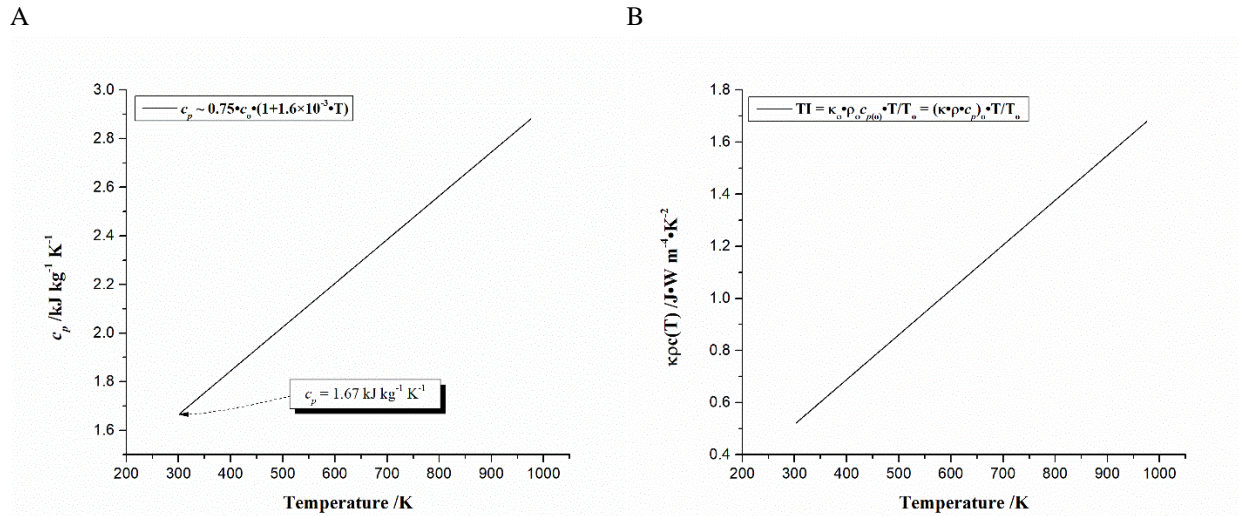
Figure 4. A. $c_p = c_p(T)$ for pyrolysis process of CBF sample. B. $\kappa \cdot \rho \cdot c(T)$ dependence (TI – thermal inertia) of CBF sample, during the pyrolysis process

Both c_p and TI increase with progresses of reaction temperature, i.e., with advancement of thermo-chemical conversion of tested material. The position of $c_p - T$ plot (approximately with ratio of 45°-45° angle, respecting to Y-X axis) corresponds to wood-based cellulose material, but this position is recognizable for the cellulose esters [39], such as CTA present in the investigated sample (c_p values increase linearly with an increasing of temperature) (fig. 4 A). The lowest value of c_p identified at room temperature amounts 1.67 kJ kg^{-1} K^{-1} which was typical value for cellulose ester fibers established [35]. Additionally, it should be mentioned that obtained results in fig. 4 A are similar with specific heat capacity behavior for amorphous D-glucose (presence of reduced crystallinity below 50%) [35]. With an increasing of the temperature, c_p noticeably rises, reaching markedly a high value (the maximum value of c_p was 2.88 kJ kg^{-1} K^{-1}) (fig. 4 A). Also, the TI value increases with an increase of the temperature (fig. 4 B), where obtained results show that the rate of material thermal transformation is linearly accelerated, whereby thermal mass and velocity of the thermal wave strongly controls the surface temperature of a material, in its thermally induced degradation. This is especially pronounced at the very end of the process, showing that created product (the manufactured solid product – bio-char) has a great capacity to store the heat (as the latent heat storage material (rich in carbon)), and this is highly dependent on the formed particles size diameter and the porosity. Fig. 5 shows the temperature dependence of the thermal conductivity (κ), for the experimental temperatures below and above the glass transition temperature (T_g).
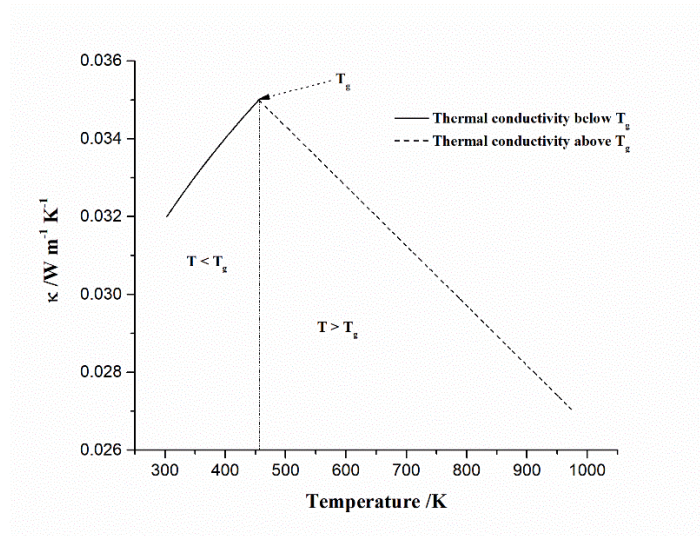
Figure 5. The temperature dependence of thermal conductivity (κ) for CBF pyrolysis process, for $T < T_g$ and $T > T_g$, respectively

It can be seen from fig. 5, that the thermal conductivity increases up to the T_g point (for $T < T_g$) which suggests that below the glass transition temperature, the amorphous polymer is a rigid solid, with ordered cellulose fibers behaving with increased conductivity. Above T_g, there is reduction in the stiffness and the change of density ρ and thermal conductivity (decreases behavior against the temperature), indicating an dramatic change in stiffness (at T_g) between the glassy state and the rubbery or the fluid state (fig. 5). If the monomer sequence is fairly regular and symmetric, the polymer chain can crystallize into ordered domains known as crystallites, which are dispersed in the amorphous (disordered) polymer. At the melting temperature T_m (~ 258.50 ^{o}C, where it is located within the $T > T_g$ region), the cellulose acetate crystallites melt and entire polymer becomes amorphous and then can flows. Because the melting temperature of the crystallites is above the T_g, crystallinity raises the flow temperature of the micro-plastic and makes it more rigid. However, crystallinity does not prevent flaming drips, as the melting temperature is usually much lower than the ignition temperature. Since that the investigated material has high DS value, the present CTA possesses lower T_g, thereby increasing T_m, so the pyrolysis process is complex, where melting and degradation overlaps (for a more detailed analysis, measurements in undercooling conditions should be carried out, considering the influence of plasticizer). The magnitude drops of κ after T_g (fig. 5) depends on material fibrillation. Namely, the fibrillation may increases the thermal resistance in the sample, but κ is strongly limited by inherent nano-sized structure and already existing micro-fibril boundaries, it does not affect the temperature dependence of κ, and only weakly its magnitude. For resolving of this issue, the structural studies must be implemented. These analyses can show a possible increasing of the disorder in the chain packing and hydrogen bonding outward from the center of elementary fibrils, which may further decreases the crystallite size [40].

Conclusions

The actual paper provides analysis of thermo- and thermophysical characteristics of the used cigarette butt filters (CBFs) during thermo-chemical conversion through the slow pyrolysis process. The process was

11

monitored by various thermal analysis techniques (simultaneous TG-DTG-DTA methods and DSC analysis) under non-isothermal conditions. By thermal stability properties, it was concluded that pyrolysis proceeds *via* complex multi-steps, encompassing moisture evaporation stage, plasticizer evaporation stage, thermal decomposition of cellulose triacetate (CTA), the ash-formation stage, and the bio-char production stage. The exothermic effect detected at 204.12 ^oC was attributed to cellulose ester crystallization. The latter indicated on the change in the degree of substitution – DS. Futhermore, the second exothermic effect detected at 348.84 ^oC was attached to the possible secondary crystallization arrangement, and also to recombination of the hydrogen bonding. The dipolar interactions and hydrogen bonding between plasticizer and the cellulose ester are responsible for the position of the glass transition temperature (T_g) of the blend (CTA + TAC) in the CBF sample. The sharp and narrow endothermic peak was marked at 382.14 ^oC, which is attributed to the melting of the acetylated sample, which also overlaps with the thermal decomposition process. Two other exothermic effects were also observed, attributed to the ash formation and the production of bio-char, respectively.

It was found that devolatilization index (D_i) increases with an increase in the heating rate, indicating that higher heating rate promotes release of volatiles. It was assumed that decrease of the crystallinity (i.e., semi-crystallinity attributes) indicates on the reduction of hydroxyl groups, leading to less organization of the chains, and decreasing inter-molecular interactions through hydrogen bonding. This is reflected on the values of heat-resistance index of tested material at different heating rates. The temperature dependence of the specific heat capacity (c_p) and thermal inertia (TI) during thermo-chemical conversion of CBF show an increasing linear trend with temperature, where identified dependencies are typical for cellulose ester fibers. Based on TI value at high pyrolysis temperature, it was concluded that produced bio-char has a great capacity to store the heat, depending on particles size diameter and its porosity. A sudden change in thermal conductivity was observed at T_g. The reason for this change lies in the quick physical change of the material, from its rigid form to its viscous (fluid) form. It was concluded that magnitude drops of thermal conductivity after T_g depends on material fibrillation. For a more detailed physicochemical analysis of the tested sample during its conversion, it was concluded that additional structural studies are required to be carried out for clarifications of the issues related to the thermal behavior of starting material. This will be the subject of our further research in the future.

Nomenclature

Abbreviations

CBs - cigarette butts

CAc {CA} – cellulose acetate

TAC – triacetin

PAHs - polycyclic aromatic hydrocarbons

PACs - polycyclic aromatic compounds

T_g – the glass transition temperature [^oC [K]]

T_m – the melting temperature [^oC [K]]

T_{in} - the initial devolatilization temperature [^oC]

T_{max} - the maximum mass loss temperature [^oC]

R_{max} - the maximum decomposition rate [%/min]

$\Delta T_{1/2}$ - the temperature interval when the value of

CBFs - cigarette butt filters

TG – thermogravimetry

DTG – derivative thermogravimetry

DTA – differential thermal analysis

DSC – differential scanning calorimetry

HRI – the heat-resistance index

TI – thermal inertia

CDA - cellulose diacetate

CTA – cellulose triacetate

RT – the room temperature

DS – the degree of substitution

CTA + TAC – cellulose triacetate/triacetin blend

endo – endothermic

exo – exothermic

Greek symbols

β – heating rate [K/min]

φ – the gas flowing rate [mL min^{-1}]

κ – the thermal conductivity [W m^{-1} K^{-1}]

κ_o - the thermal conductivity at the standard temperature [W m^{-1} K^{-1}]

$\kappa(T_g)$ - the thermal conductivity at the glass transition temperature [W m^{-1} K^{-1}]

ρ – the density [kg m^{-3}]

ρ_o - the density at temperature of 298 K [kg m^{-3}]

R/R_{max} was ½ [^{o}C] {*apropos* when the instantaneous mass loss rate equals to the half of R_{max}}

D_i – the devolatilization index [%·min^{-1}·C^{o-3}]

T_o – the standard temperature [K]

ΔT – the temperature range [K]

T_5 – the temperature at 5% of mass loss of the sample [^{o}C]

T_{30} – the temperature at 30 % of mass loss of the sample [^{o}C]

B - the volume thermal expansivity *per* the unit mass [m^3 kg^{-1} K^{-1}]

c_o (or $c_{p(o)}$) - the heat capacity at the standard temperature [kJ kg^{-1} K^{-1}]

c_p - the heat capacity [kJ kg^{-1} K^{-1}]

Δc_p - the change in heat capacity at the glass transition temperature [kJ kg-1 K-1]

T_{HRI} – the heat-resistance index [^{o}C]

References

[1] Ng, M., Freeman, M.K., Fleming, T.D., *et al.*, Smoking Prevalence and Cigarette Consumption in 187 Countries, 1980-2012, *Jama*, *311* (2014), 2, pp. 183-192.

[2] Mackay, J., Eriksen, M., Shafey, O., The Tobacco Atlas, 2nd Ed., Atlanta, Georgia, American Cancer Society, (2006), pp. 1-128.

[3] Curtis, C., Novotny, T.E., Lee, K., Freiberg, M., McLaughlin, I., Tobacco industry responsibility for butts: A model tobacco waste act, *Tobacco Control*, *26* (2017), 1, pp. 113-117.

[4] Marinello, S., Lolli, F., Gamberini, R., Rimini, B., A second life for cigarette butts? A review of recycling solutions, *Journal of Hazardous Materials*, *384* (2020), p. 121245. https://doi.org/10.1016/j.jhazmat.2019.121245

[5] Smith, E.A., McDaniel, P.A., Covering their butts: Responses to the cigarette litter problem, *Tobacco Control*, *20* (2011), 2, pp. 100-106.

[6] Novotny, T.E., Lum, K., Smith, E., Wang, V., Barnes, R., Cigarettes butts and the case for an environmental policy on hazardous cigarette waste, *International Journal of Environmental Research and Public Health*, *6* (2009), 5, pp. 1691-1705.

[7] Kabir, G., Hameed, B.H., Recent progress on catalytic pyrolysis of lignocellulosic biomass to high-grade bio-oil and bio-chemicals, *Renewable and Sustainable Energy Reviews*, *70* (2017), pp. 945-967. https://doi.org/10.1016/j.rser.2016.12.001

[8] Sayers, E.W., Barrett, T., Benson, D.A., *et al*., Database resources of the National Center for Biotechnology Information, *Nucleic Acids Research*, *39* (2011), 1, pp. D38-D51. https://doi.org/10.1093/nar/gkq1172

[9] Lam, S.S., Liew, R.K., Wong, Y.M., Azwar, E., Jusoh, A., Wahi, R., Activated carbon for catalyst support from microwave pyrolysis of orange peel, *Waste and Biomass Valorization*, *8* (2017), pp. pages 2109-2119.

[10] Long, Y., Chua, Y.W., Wu, H., Acid-catalysed cellulose pyrolysis at low temperatures, *Fuel*, *193* (2017), pp. 460-466.

[11] Al Shra'ah, A., Helleur, R., Microwave pyrolysis of cellulose at low temperature, *Journal of Analytical and Applied Pyrolysis*, *105* (2014), pp. 91-99.

[12] Zhang, X., Li, J., Yang, W., Blasiak, W., Formation mechanism of levoglucosan and formaldehyde during cellulose pyrolysis, Energy Fuels, *25* (2011), 8, pp. 3739-3746.

[13] Sharuddin, S.D.A., Abnisa, F., Daud, W.M.A.W., Aroua, M.K., Pyrolysis of plastic waste for liquid fuel production as prospective energy resource, *IOP Conference Series: Materials Science and Engineering*, *334* (2018), p. 012001. DOI 10.1088/1757-899X/334/1/012001

[14] Novotny, T.E., Zhao, F., Consumption and production waste: another externality of tobacco use, *Tobacco Control*, *8* (1999), 1, pp. 75-80.

[15] Slaughter, E., Gersberg, R.M., Watanabe, K., Rudolph, J., Stransky, C., Novotny, T.E., Toxicity of cigarette butts, and their chemical components, to marine and freshwater fish, *Tobacco Control*, *20* (2011), 1, pp. i25-i29.

[16] Dobaradaran, S., Nabipour, I., Saeedi, R., *et al*., Association of metals (Cd, Fe, As, Ni, Cu, Zn and Mn) with cigarette butts in northern part of the Persian Gulf, *Tobacco Control*, *26* (2017), 4, pp. 461-463.

[17] Chevalier, Q., El Hadri, H., Petitjean, P., *et al*., Nano-litter from cigarette butts: Environmental implications and urgent consideration, *Chemosphere*, *194* (2018), pp. 125-130.

[18] Green, A.L.R., Putschew, A., Nehls, T., Littered cigarette butts as a source of nicotine in urban waters, *Journal of Hydrology*, *519* (2014), Part D, pp. 3466-3474.

[19] Ogundare, S.A., Moodley, V., Werner, E.V.Z., Nanocrystalline cellulose isolated from discarded cigarette filters, *Carbohydrate Polymers*, *175* (2017), pp. 273-281.

[20] Huang, F., Xu, Y., Peng, B., Su, Y., Jiang, F., Hsieh, Y.-L., Wei, Q., Coaxial electrospun cellulose-core fluoropolymer-shell fibrous membrane from recycled cigarette filter as separator for high performance lithium-ion battery, *ACS Sustainable Chemistry & Engineering*, *3* (2015), 5, pp. 932-940.

[21] Bridgwater, A.V, Peacocke, G.V.C., Fast pyrolysis processes for biomass, *Renewable and Sustainable Energy Reviews*, *4* (2000), 1, pp. 1-73.

[22] Demirbas, A., Arin, G., An overview of biomass pyrolysis, *Energy Sources*, *24* (2002), 5, pp. 471-482.

[23] Meng, H., Wang, S., Chen, L., Wu, Z., Zhao, J., Thermal behavior and the evolution of char structure during co-pyrolysis of platanus wood blends with different rank coals from northern China, *Fuel*, *158* (2015), pp. 602-611.

[24] Hafiezal, M.R.M., Khalina, A., Zurina, Z.A., Azaman, M.D.M., Hanafee, Z.M., Thermal and flammability characteristics of blended Jatropha bio-epoxy as matrix in carbon fiber-reinforced polymer, *Journal of Composites Science*, *3* (2019), p. 6. doi:10.3390/jcs3010006

[25] Bicerano, J., Prediction of Polymer Properties, 2nd Edition, Marcel Dekker, Inc., New York, 1996.

[26] Van Krevelen, D.W., Properties of Polymers, 3rd Edition, Elsevier Scientific, New York, 1990.

[27] Kamide, K., Saito, M., Thermal analysis of cellulose acetate solids with total degrees of substitution of 0.49, 1.75, 2.46 and 2.92, *Polymer Journal*, *17* (1985), pp. 919-928.

[28] Kamide, K., Okajima, K., Kowsaka, K., Matsui, T., Nomura, S., Hikichi, K., Effect of the distribution of substitution of the sodium salt of carboxymethylcellulose on its absorbency toward aqueous liquid, *Polymer Journal*, *17* (1985), pp. 909-918.

[29] Bao, C.Y., Cellulose acetate/plasticizer systems: structure, morphology and dynamics, Polymers. Université Claude Bernard - Lyon I, 2015. English, NNT: 2015LYO10049, Available at: https://theses.hal.science/tel-01186696.

[30] Yousef, S., Eimontas, J., Striūgas, N., Praspaliauskas, M., Abdelnaby, M.A., Pyrolysis kinetic behaviour, TG-FTIR, and GC/MS analysis of cigarette butts and their components, *Biomass Conversion and Biorefinery*, 2022. https://doi.org/10.1007/s13399-022-02698-5

[31] De Fenzo, A., Giordano, M., Sansone, L., A clean process for obtaining high-quality cellulose acetate from cigarette butts, *Materials*, *13* (2020) pp. 4710. doi:10.3390/ma13214710.

[32] Polarz, S., Smarsly, B., Schattka, J.H., Hierachical porous carbon structures from cellulose acetate fibers, *Chemistry of Materials*, *14* (2002), 7, pp. 2940-2945.

[33] Koochaki, C.B., Khajavi, R., Rashidi, A., Mansouri, N., Yazdanshenas, M.E., The effect of pre-swelling on the characteristics of obtained activated carbon from cigarette butts fibers, *Biomass Conversion and Biorefinery*, *10* (2020), 2, pp. 227-236.

[34] Barud, H.S., de Araújo Júnior, A.M., Santos, D.B., *et al.*, Thermal behavior of cellulose acetate produced from homogeneous acetylation of bacterial cellulose, *Thermochimica Acta*, *471* (2008) pp. 61-69.

[35] Hatakeyama, T., Hatakeyama, H., Thermal Properties of Cellulose and its Derivatives – Ch. 3, In: Thermal Properties of Green Polymers and Biocomposites. Part of the book series: Hot Topics in Thermal Analysis and Calorimetry (HTTC, Vol. 4), Springer, Kluwer Academic Publishers, 2004, pp. 39-130.

[36] Li, X., He, F., Su, X., *et al.*, Evaporation rate of potassium chloride in combustion of herbaceous biomass and its calculation, *Fuel*, *257* (2019) pp. 116021. https://doi.org/10.1016/j.fuel.2019.116021

[37] Erdmann, R., Kabasci, S., Heim, H.-P., Thermal properties of plasticized cellulose acetate and its β-relaxation phenomenon, *Polymers*, *13* (2021), 9, pp. 1356. https://doi.org/10.3390/polym13091356

[38] Wolfs, J., Meier, M.A.R., A more sustainable synthesis approach for cellulose acetate using the DBU/CO_2 switchable solvent system, *Green Chemistry*, *23* (2021) pp. 4410-4420.

[39] Hatakeyama, T., Nakamura, K., Hatakeyama, H., Studies on heat capacity of cellulose and lignin by differential scanning calorimetry, *Polymer*, *23* (1982) pp. 1801-1804.

[40] Fernandes, A.N., Thomas, L.H., Altaner, C.M., *et al.*, Nanostructure of cellulose microfibrils in spruce wood, *Proceedings of the National Academy of Sciences of the United States of America*, *108* (2011), 47, pp. E1195-E1203.